Temperature of zenith mask

Zenith mask temperature is measured by two sensors; another sensor measures the temperature of the motor which actuates mask status (open/close). In the following we show how the temperature changes during the flight (Fig. 1, lower curve is the motor temperature, upper curves are mask temperatures); note that the two sensors on the mask overlap (as expected). The extremely good correlation between the two sensors is well shown also in Fig. 2. Correlation between the average mask temperature and the motor temperature is not so good (Fig. 3). Please note that during the flight the mask was always kept closed even if the motor received commands for opening/closing the shutter.

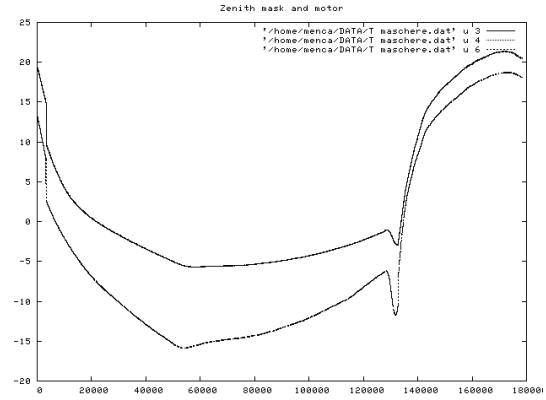

Illustration 1 Z. mask and motor

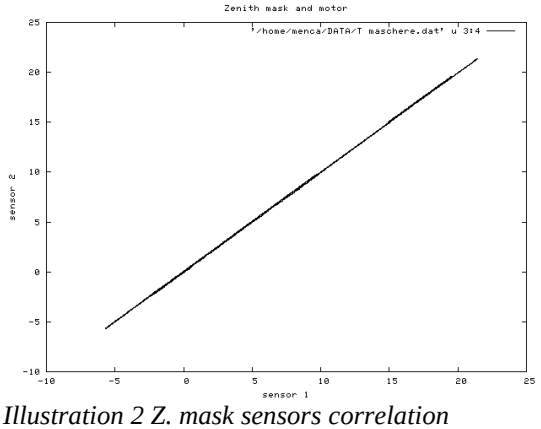

Illustration 2 Z. mask sensors correlation

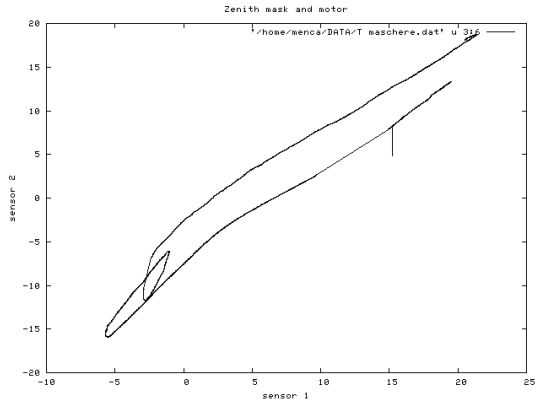

Illustration 3 Z. mask / motor correlation

Temperature of atmospheric mask

The behavior of atmospheric mask is more complex that the one of the zenith mask; first of all let us note that (Fig. 4) the mask sensors show a *bump* starting at about 6.86 hours and ending at about 8.03 (time as transmitted by CEU). The reason of this sudden change (20 degrees up in 35 minute and then 20 degrees down in the same time) has not yet been understood, but a possibility is the sunrise. In this case however we must suppose that the gondola was for some reason oriented towards East and not towards North. **This should be checked as soon as the data from the ACS system will be available**. Note also (Fig. 5) that the two sensors on the mask show a correlation poorer that the one we have seen for the zenith mask; same poorer correlation appears when we compare the average mask temperature and the motor temperature (Fig. 6). Lack of correlation is mainly due to what happens during the *bump;* **this suggests that different parts of the mask get heated in different way and that the thermal conductivity is not high enough to distribute head evenly within this time constant**. If we drop data inside this region the correlation between mask sensors is significantly better (Fig. 7) and the correlation between mask and motor (Fig. 8) is not significantly poorer than the one we have found for the zenith mask/motor. As a comparison I have also plotted the correlation between mask sensors (Fig. 9) and motor inside bump (Fig. 10, note the change of scale).

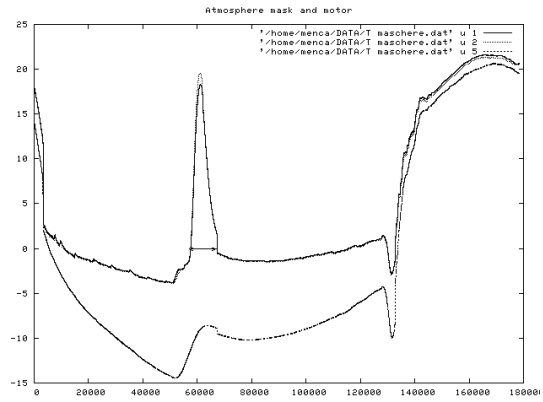

Illustration 4 A. mask and motor temperature

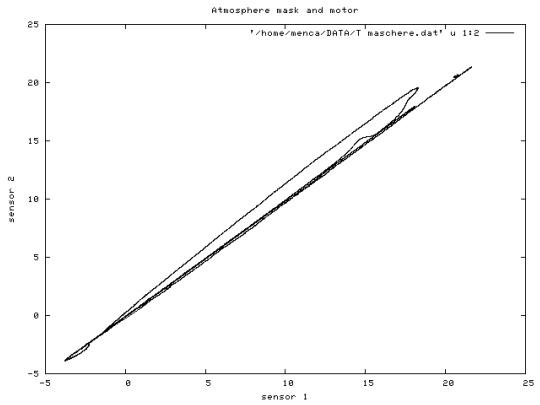

Illustration 5 A. mask sensors correlation

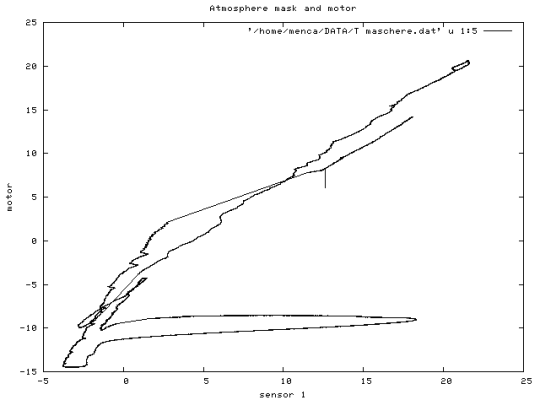

Illustration 6 A. mask average and motor correlation

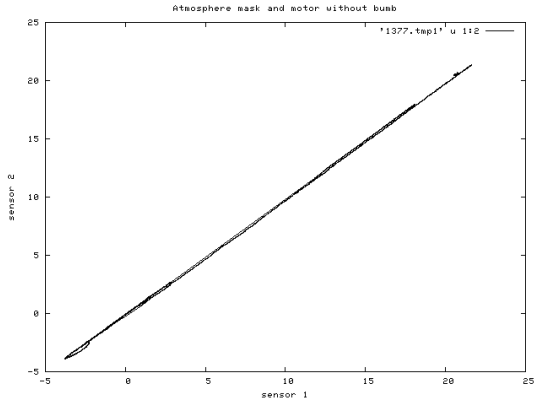

Illustration 7 A. sensors outside bump correlation

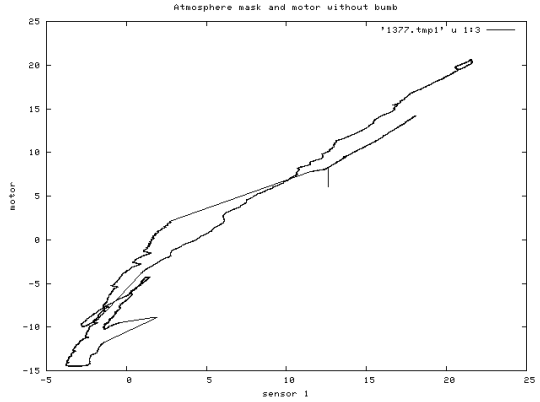

Illustration 8 A. mask average and motor correlation outside bump

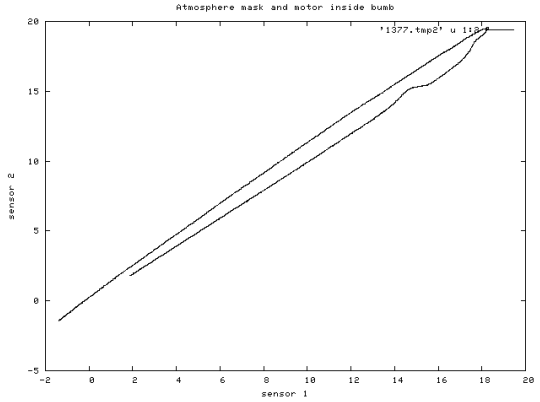

Illustration 9 A. mask sensor correlation inside bump

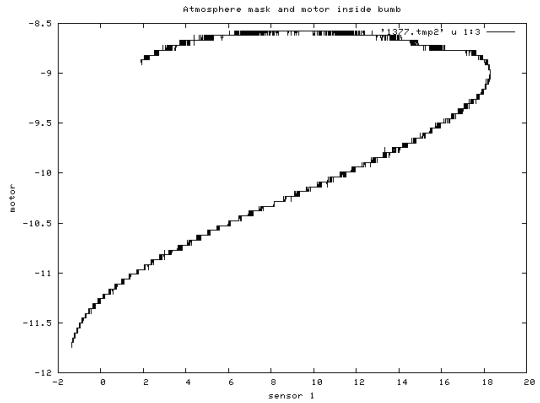

Illustration 10 A. mask and motor inside bump

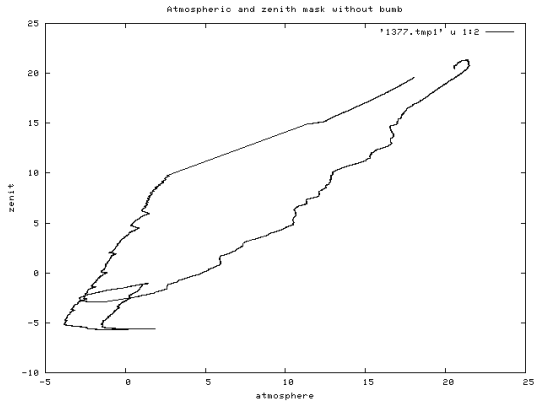

Illustration 11 A. and Z. mask outside bump

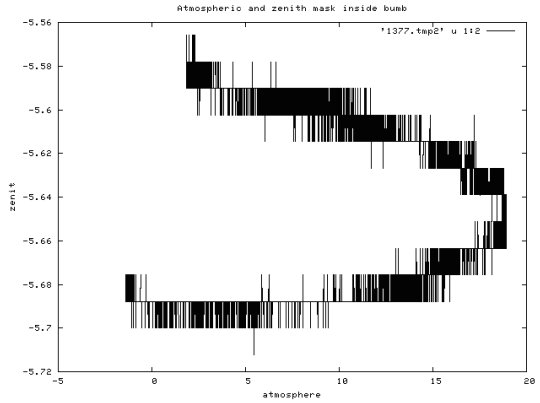

Illustration 12 A. and Z. mask inside bump

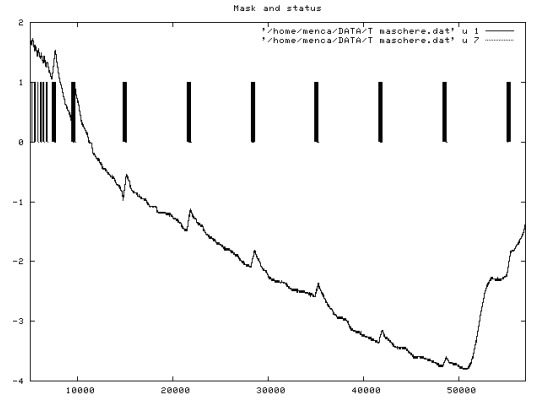

Illustration 13 A. mask temperature and status

For completeness I have finally plotted the correlation between average temperature on the two masks (Fig. 11 and Fig. 12). Finally note the small change of temperature that the atmospheric mask undergoes when the mask is closed (vertical bars, Fig. 13). This is due to the fact that temperature inside the instrument is higher that outside and therefore the mask is hotter when closed.

Temperature inside the instrument

Temperature inside the instrument is measured by two sensors, one placed on the *pagoda* and one placed on the brake motor. As shown in Fig. 14 temperature never goes below -6 C; also the pagoda at about 7.00 hours starts heating faster than the motor; this may be expected because the pagoda is oriented East[1]. Note also that at about 16.00 hours the pagoda temperature has a sudden drop and goes to the minimum (-26 C); this suggests that a problem in the conversion has developed. **We need to check whether the pagoda temperature is converted by SAP electronics (or by CEU) and verify if the same happens for all housekeepings converted by the same device.** An excerpt of the same data (where the beginning and the end have been cut) is shown in Fig. 15, while in Fig. 16 the data are shown during the ascension phase.

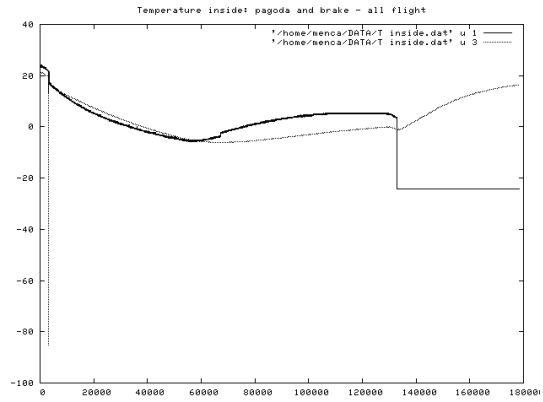

Illustration 14 Pagoda and Brake temperature

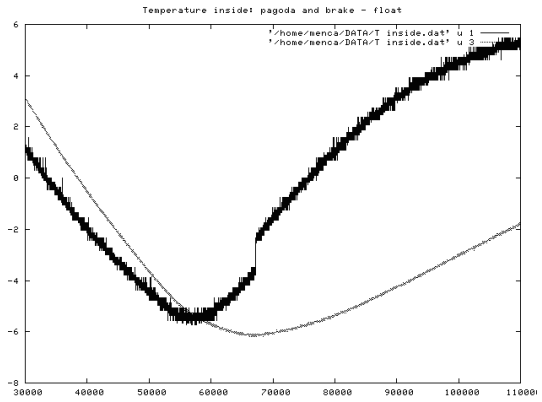

Illustration 15 Pagoda and brake temperature (section)

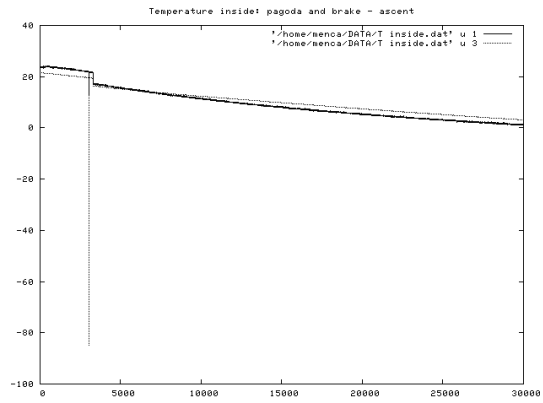

Illustration 16 Pagoda and brake during ascent

1 But see above, pag. 2, about possible problems in gondola orientation

Laser correction

Information on laser stability comes as correction applied to keep constant temperature. The data for all the flight are shown in in Fig. 17[2]; note the behavior in the last part of recording, Stability during the float part of the flight is shown in Fig. 18; some instabilities appear only immediately after power on as shown in Fig. 19)

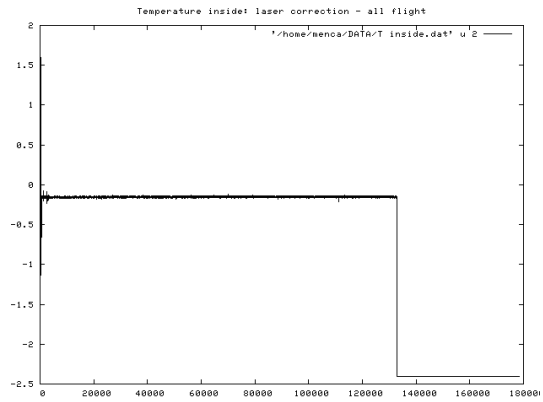

Illustration 17 Laser correction

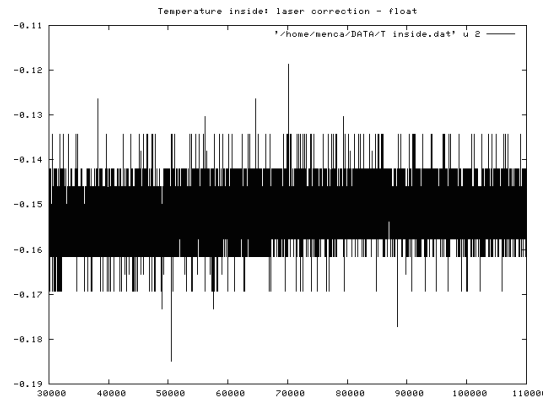

Illustration 18 Laser correction (section)

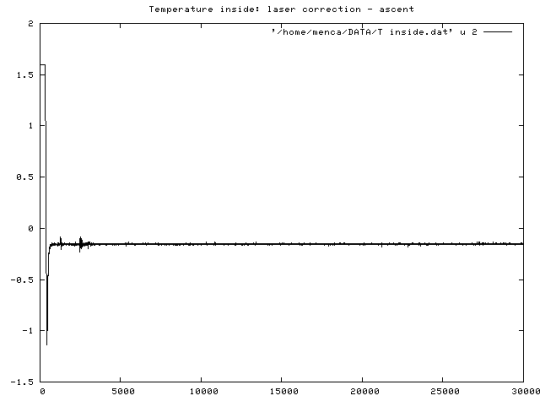

Illustration 19 Laser correction during ascension phase

It may be interesting to understand if the laser correction in completely random of if there are resonances. What I have done is to evaluate the power spectrum using a standard GNU program (lomb.c); final result is shown in Fig. 20) The sampling frequency (one value for each major frame, 2.37[3] hz) suggests a Nyquist frequency of 1.185 hz. Note the presence of a small feature at about at about 0.5 hz which is near, but anyway clearly different from, half Nyquist frequency[4]. The same spectrum (in a log/log plot) is shown in Fig. 21 which clearly shows that no peak resonances are present.

As a further check I have also estimated the power spectrum using the maximum

2 Note the beaviour at the end of recorded data; this is the same as already seen in pag. 4

3 65536/(108*256), where 65536 is the bit/sec rate, 256 is the number of bit per minor frame and 108 is the number of minor frames per major frame.

4 This frequency appears often in the power spectra; this suggests that it is probably due to electronics and not to physical effects.

entropy method (memse.c). Looking at Fig. 22, it is immediately evident that the noise is by far smoothed out and that the feature is much more prominent. The position of the feature as found by memse is in excellent agreement with the one suggested by lomb (Fig. 23). The smoothness of the memse spectrum is clearly related to a *redistribution* of the power within the spectrum bins (Fig. 24)

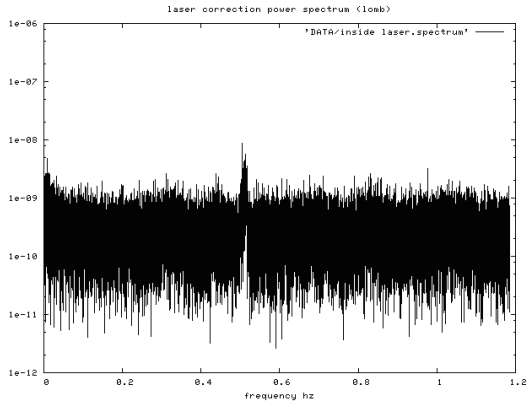

Illustration 20 Power spectrum of laser correction

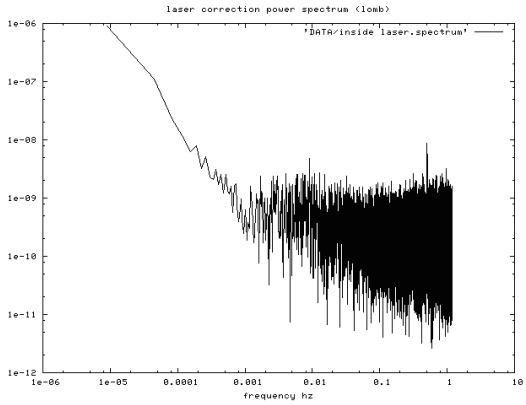

Illustration 21 Power spectrum of laser correction

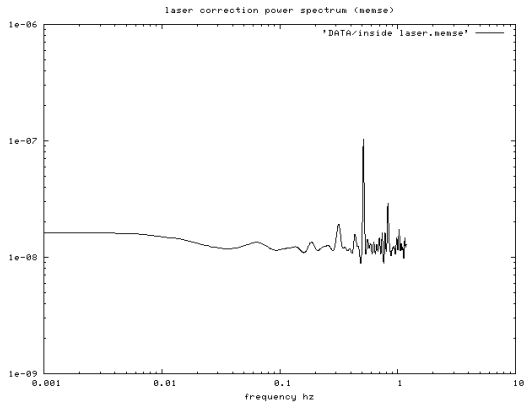

Illustration 22 Maximum entropy spectrum of laser correction

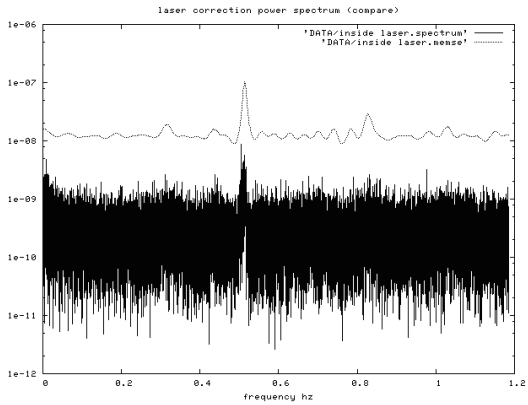

Illustration 23 Compare power and maximum spectra of laser correction

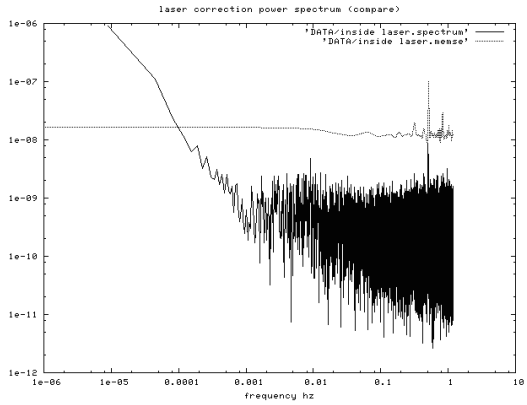

Illustration 24 Compare maximum entropy and power spectra of laser correction

Temperature outside

Temperature outside the instrument has been evaluated using two sensors; the air temperature sensor is a free standing sensor within the gondola, the output port sensor is a sensor glued to the instrument near the polarizing beam splitter. As a comparison the value from the two sensor have been plotted with the measurements from the masks. Note that the output port temperature is halfway between the masks temperatures (Fig. 26 and 28), while the air sensor clearly shows faster heating in the morning (after sunrise) than any of the masks (Fig. 25 and 27).

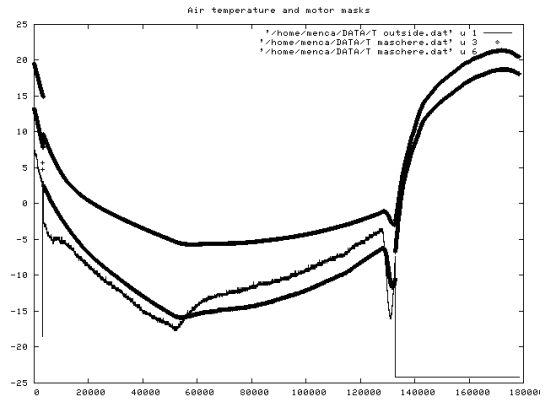

Illustration 25 Air and masks temperature

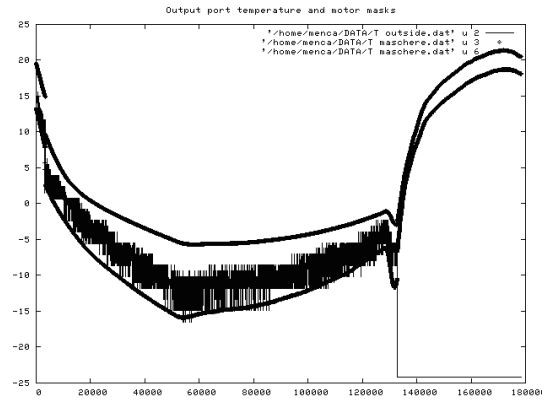

Illustration 26 Out port and masks temperature

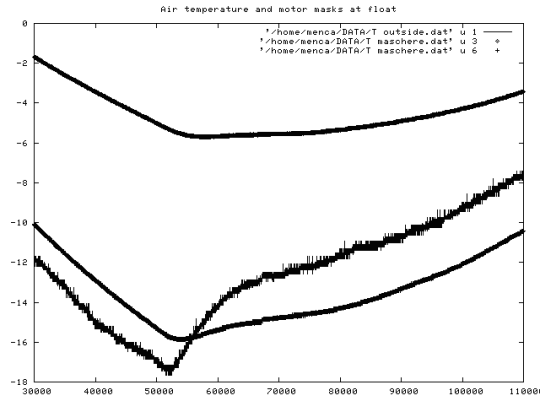

Illustration 27 Air and masks temperature

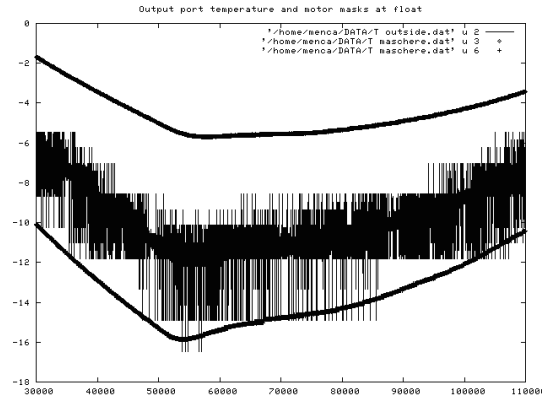

Illustration 28 Out port and masks temperature

Sap temperatures

The SAP has two temperature sensors, one for the inclinometer and one for the shaft encoder. Measurements for the two sensors are shown in Fig. 29[5] and 30). We have also shown in Fig. 29 the range of temperature where the automatic switch on/off of the heaters take place; the measurements are always above this value and this explains why we never have seen the heaters working. Correlation between the two sensors is shown in Fig. 31.

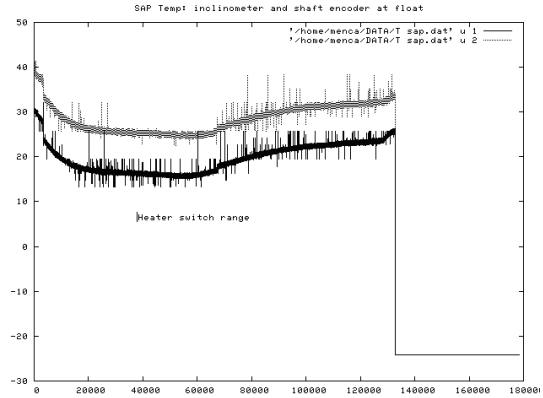

Illustration 29 Inclinometer ans SAE temperature

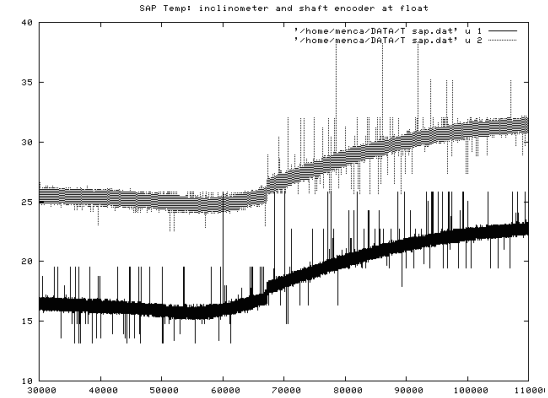

Illustration 30 Inclinometer and SAE temperature

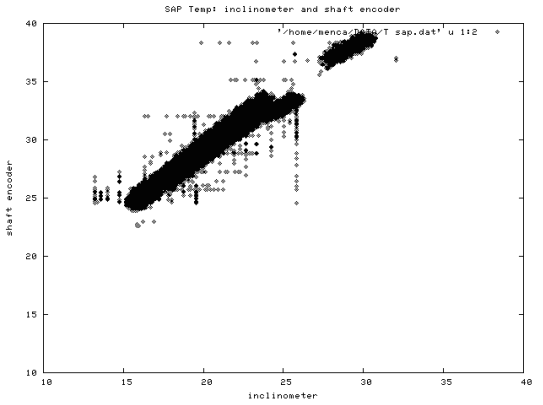

Illustration 31 SAE and Inclinometer temp. correlation

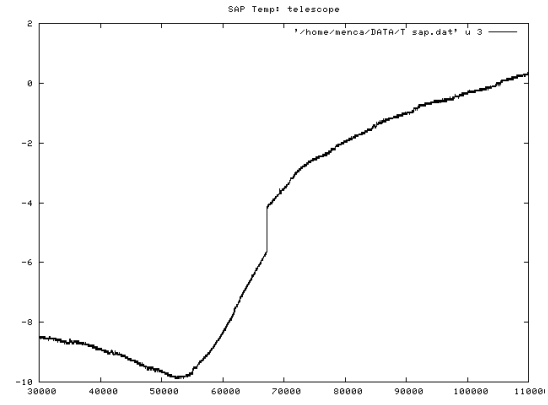

Illustration 32 Telescope temperature

For completeness I have also plotted here the temperature of the telescope; note that is the coldest place of the instrument (always below 0 C).

5 Note again that, as seen in pag. 4, there are problems after cut down

Pressure

Pressure values are shown unconverted because the balloon altitude is now obtained from GPS measurements (Pg 11). The instrument has three sensors with different working ranges: (1) sodeme, (2) sensotec, (3) baratron.; values are shown in 33 where one can see also the 'out-of-range' values for sensors 2 and 3. In the same figure I have also shown as a bar the region which I will consider as 'float', that is the region with more or less constant altitude; behavior at float is better seen in Fig. 34 and 35.

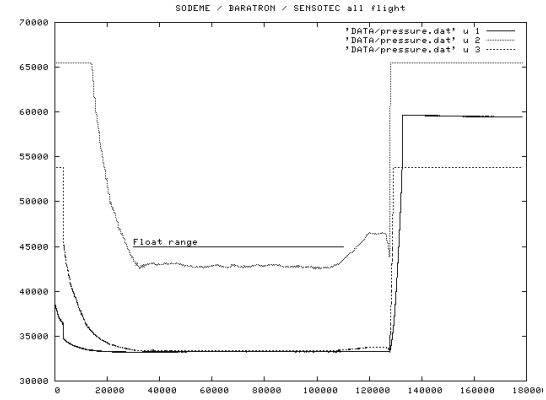

Illustration 33 Pressure during the flight

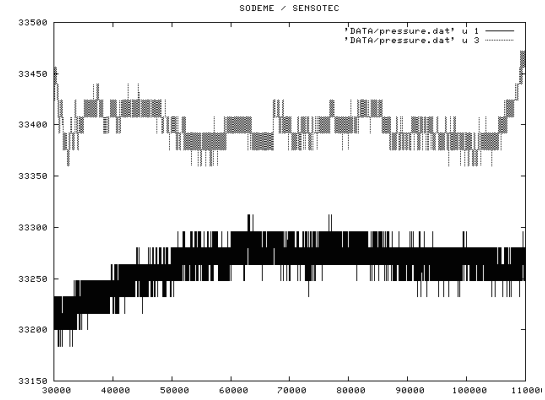

Illustration 34 Sodeme/Sensotec at float

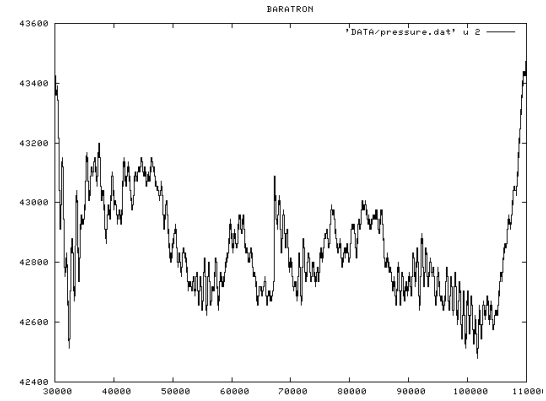

Illustration 35 Baratron at float

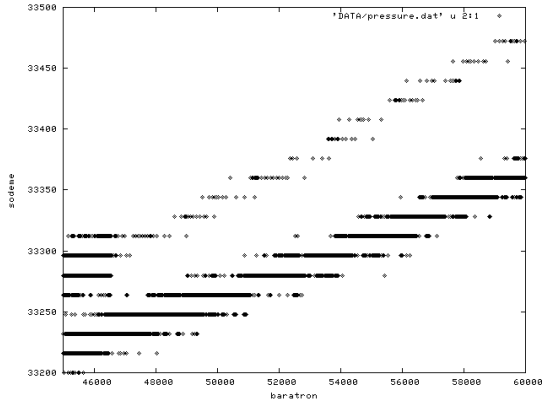

Illustration 36 Baratron/Sodeme correlation

Correlation between the different pressure sensors are shown in following figures. From Fig 36 we see that the correlation between baratron (then most accurate sensor) and sodeme (the most coarse one) is poor; the 'double line' aspect is probably due to some hysteresis in the sodeme sensor.

Fig 37 shows correlation between baratron and sensotec which is by far better even if some oscillation are present. Correlation between sensotec and sodeme is good (Fig 38) but for the 'out of range' condition for sensotec.

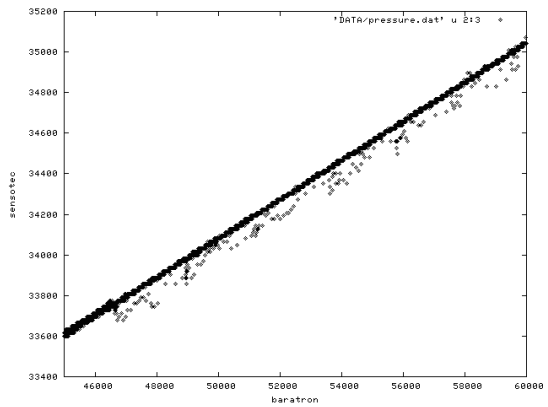

Illustration 37 Baratron/Sensotec correlation

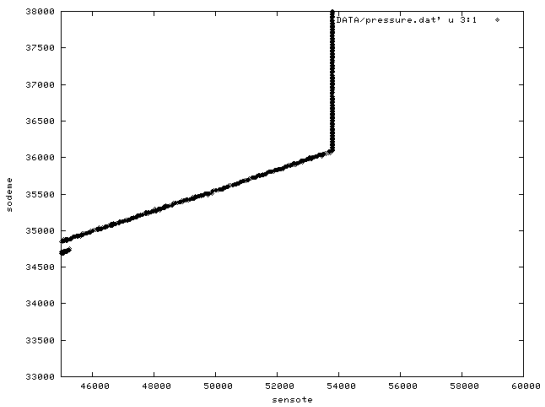

Illustration 38 Sensotec/Sodeme correlation

Fluctuation of baratron signal at float have been analyzed both with maximum spectral entropy (Fig 39) and power spectrum (Fig. 40). The two estimates are compared in Fig. 41. Note the several peaks in the power spectrum which do not appear in the maximum entropy estimate.

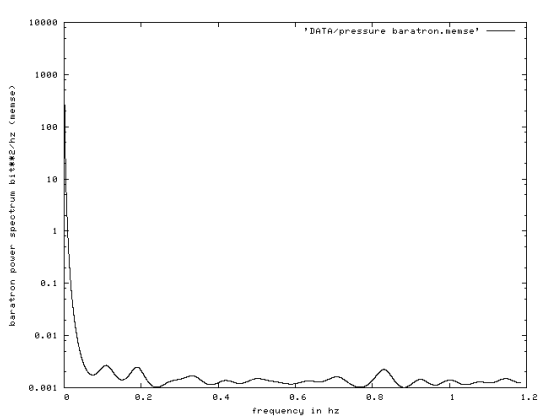

Illustration 39 Maximum entropy spectrum of baratron fluctuation

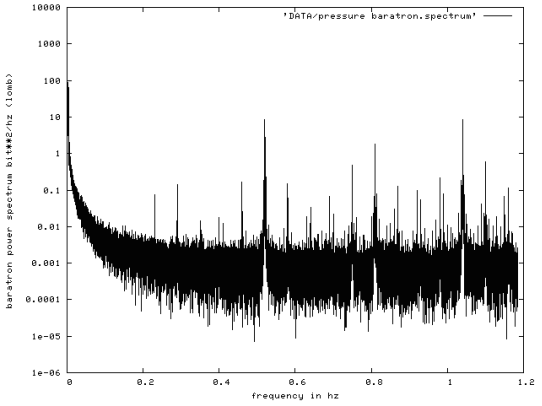

Illustration 40 Power spectrum of baratron fluctuation

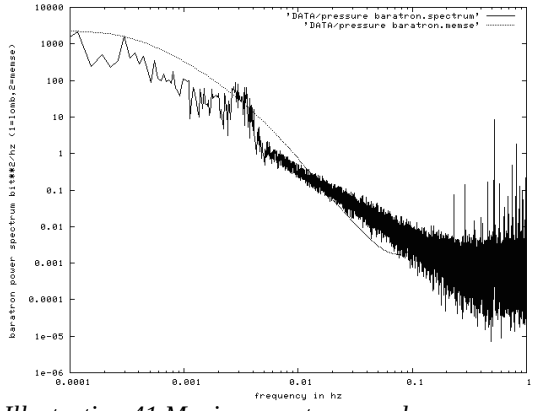

Illustration 41 Maximum entropy and power spectra comparison

GPS

Data from GPS must be considered as preliminary because the only one we have up to now are those recorded in Milo. They have not been cleaned and are therefore full of errors. Some hand cleaning has been done and results are shown below.

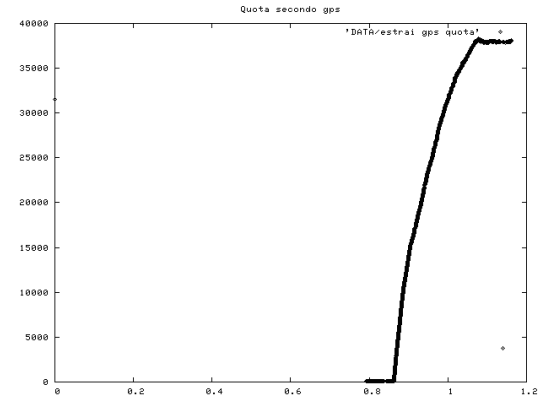

Illustration 42 Height from GPS

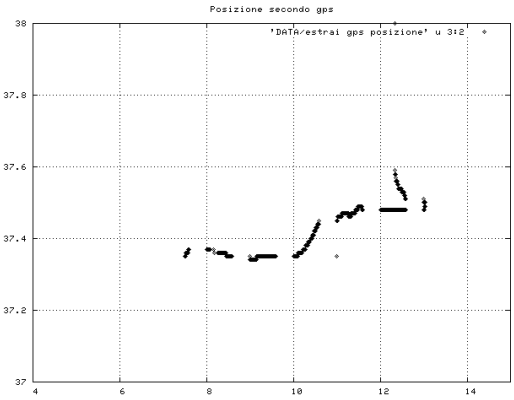

Illustration 43 Trajectory from GPS

TIME

Time returned from CEU has been converted from ASCII strings to float data (zero time assumed at 00h 29.07.02). As expected (Fig. 44) the returned values are ok. There is a sudden jump at midnight (no correction wad done in conversion for the new day). Also, since the major frames occur at 2.37 hz and the clock resolution (in the telemetry stream) is 1 second, the same value may be repeated several times as showm in the second part of the table below.

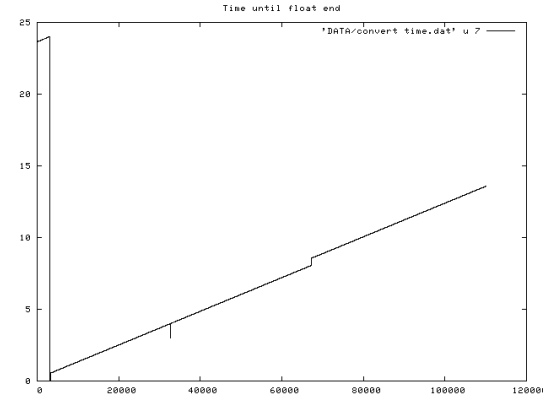

Illustration 44 Time as returned from CEU

Longest segment with same timing is 3 repeat wide

63576 values at the ending boundary of a second have been found

45625 values repeated once within one second have been found

9 values repeated twice within one second have been found

11 values repeated thrice within one second have been found

For a grand total of 110000 records

Timing difference for truely different times:
average = 1.000129 rms = 0.011511

Shuttle

The current drawn by the moving mirror carriage is shown in Fig. 45[6]; an enlarged view is shown in Fig. 46. Note that the sign is always negative (that is the sign does not carry information on the movement direction) and oscillates around -5 Amp. The oscillation follows the movement direction (upper curve in the same Fig. 46). The power spectrum of the current oscillations clearly shows a peak at the frequency corresponding to the scan period (forward/reverse) and its harmonics (Fig. 47). For completeness I have also shown in Fig. 48 the power spectrum of current fluctuation together with the power spectrum of the signal from the Lucas inclinometer which senses the angular displacement fro horizontal along the instrument axis. Note the agreement of the main frequency position (Fig. 49) and the lack of harmonics in the inclinometer signal.

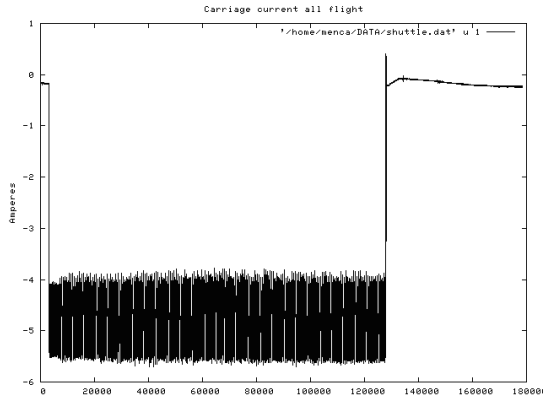

Illustration 45 Shuttle current (all flight)

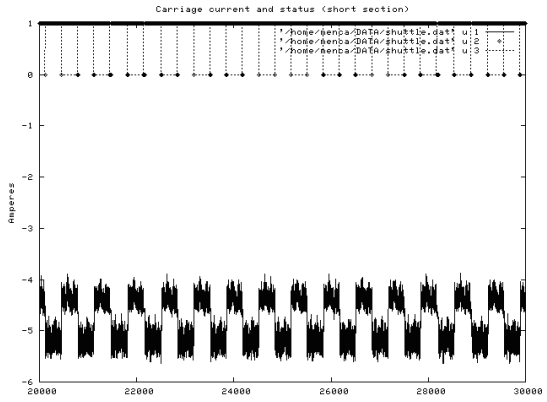

Illustration 46 Shuttle current and status (section)

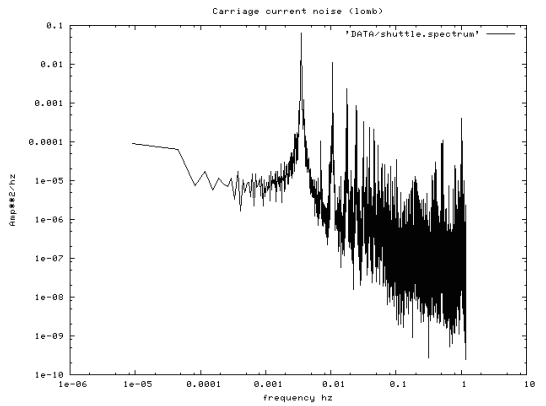

Illustration 47 Shuttle current fluctuation; power spectrum

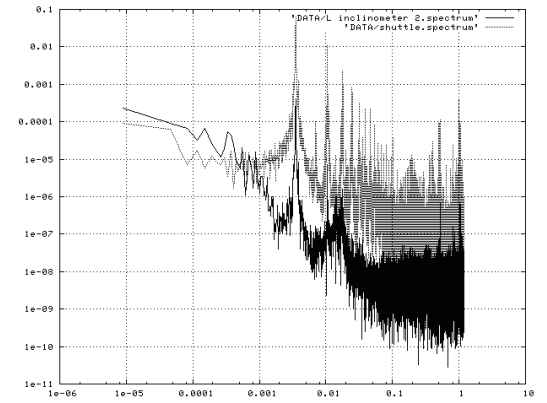

Illustration 48 Shuttle current and Lucas inclinometer power spectra

6 Note that after cut down the mirror stops moving and current go to 0

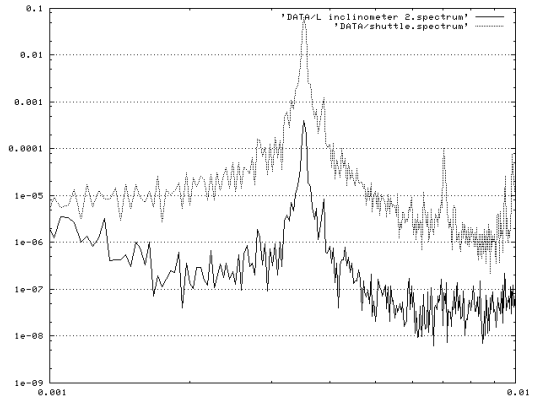

Illustration 49 Shuttle current and Lucas Inclinometer power spectra

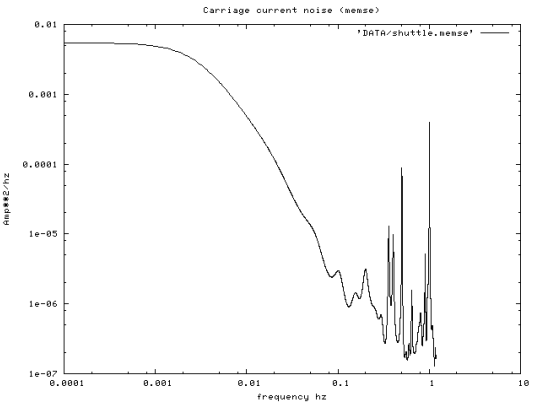

Illustration 50 Shuttle current fluctuations; maximum entropy

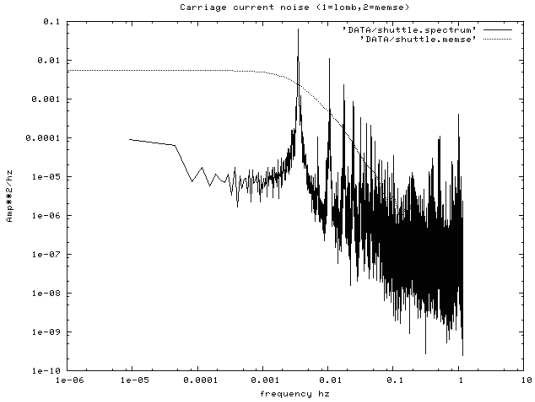

Illustration 51 Shuttle fluctuation: comparison of power spectrum and maximum entropy

The power spectrum has been also evaluated using the maximum spectral entropy method (Fig, 50) but apparently no peak is detected as better seen in Fig. 51. **This must be checked**

Lucas inclinometers

The deviation of the gondola baseplate from the horizontal are measured (coarsly) by two sensors; since we use them as raw sensors and mainly to evaluate changes they have not been calibrated[7]. The measurements for all the flight are shown in Fig. 52. Note that at the end there is clear evidence of the descent phase (oscillation) and of the 'ground' phase(constant value); note also that during the ground period the inclinometers were still performing (one of the is not out of range).
Values during the float are shown in Fig. 53 and, expanded, in Fig. 54).

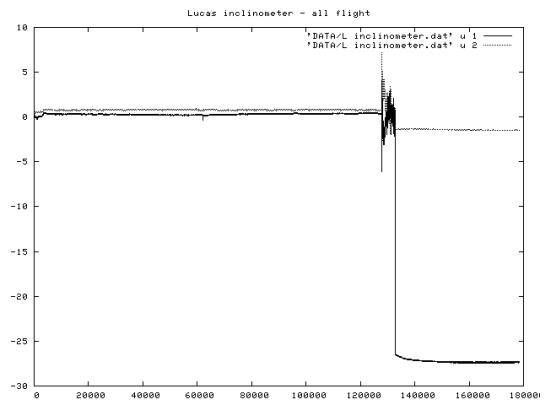

Illustration 52 Lucas Inclinometers - all flight

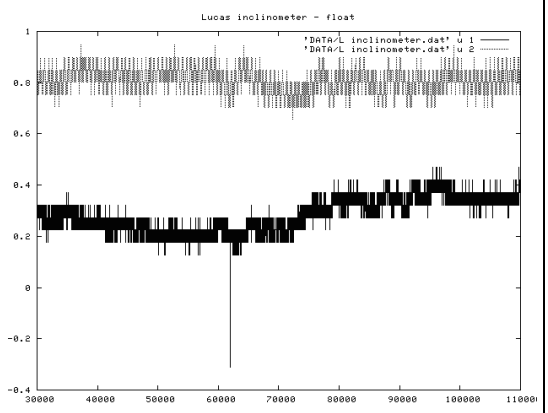

Illustration 53 Lucas inclinometers - float

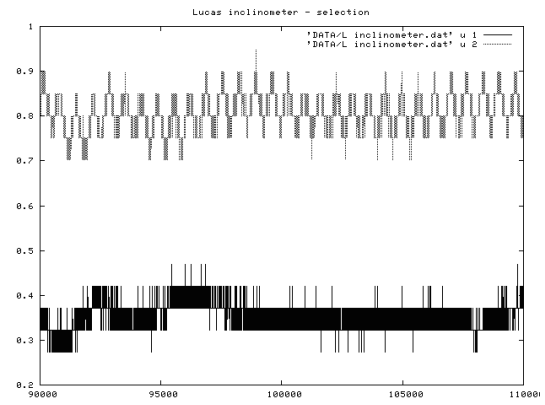

Illustration 54 Lucas inclinometers - section

From previous figures it is evident that one of the two inclinometers (number 2 in our notation) displays an oscillation. This has to be expected because the moving mirror will change the barycenter position causing the gondola to oscillate (see also pag. 12). The power spectrum of the oscillation has been evaluated for both inclinometers (Fig. 55 and 56). Note the extra peak already seen in other occasion, pag. 5. Comparison of the two spectra on a log/log scale which enhances low frequencies clearly shows the peak at the scan frequency already seen above.

7 Note also that since the horizontal (gondola level) is done making horizontal the pivot plane and not the instrument plane, any calibration needs evaluation of an offset ...

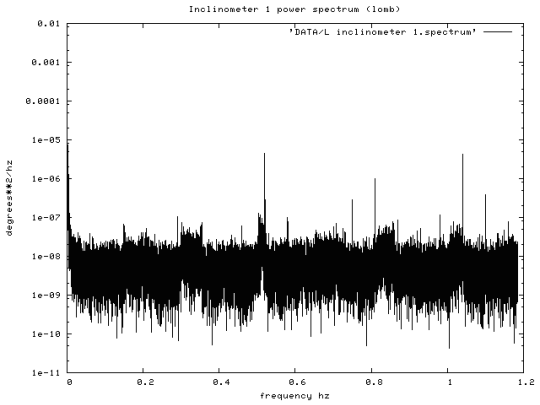

Illustration 55 Lucas inclinometer 1 - power spectrum

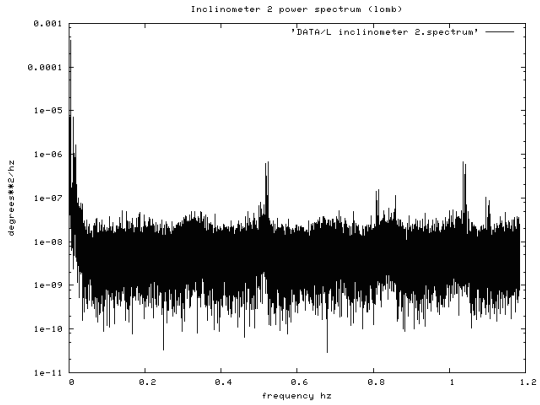

Illustration 56 Lucas inclinometer 2 - power spectrum

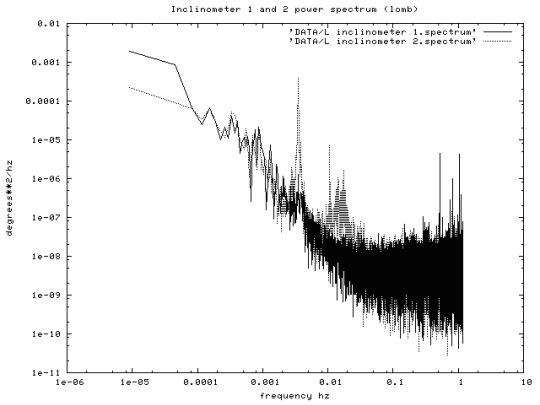

Illustration 57 Lucas inclinometers - comparison

Power spectrum evaluated using maximum spectral entropy does not show peaks (fig. 58, 59 and 60); this closely resembles what we have seen analyzing the current drawn by the mirror.

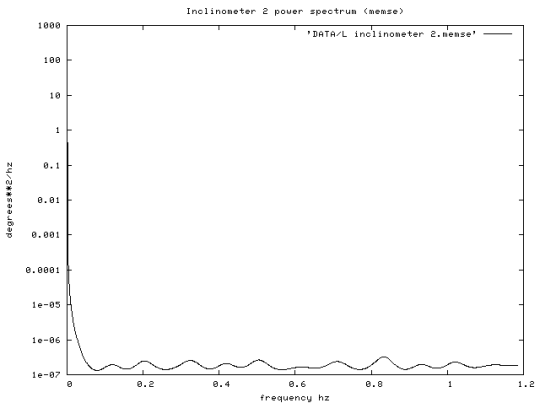

Illustration 58 Lucas inclinometer 1 - maximum entropy

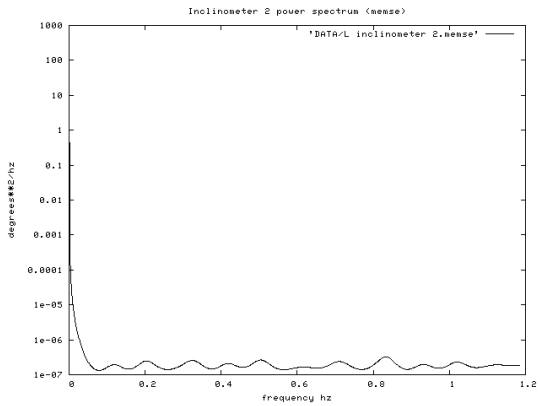

Illustration 59 Lucas inclinometer 2 - maximum entropy

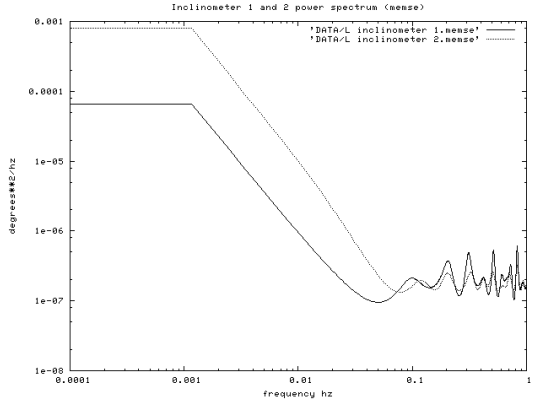

Illustration 60 Lucas inclinometers - maximum entropy comparison

Difference between power spectra and maximum spectral entropy evaluation is best seen in Fig. 61 and 62)

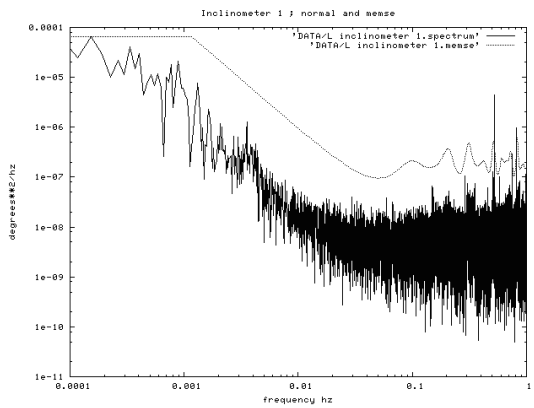

Illustration 61 Lucas inclinometer 1 - comparison of power spectrum and maximum entropy

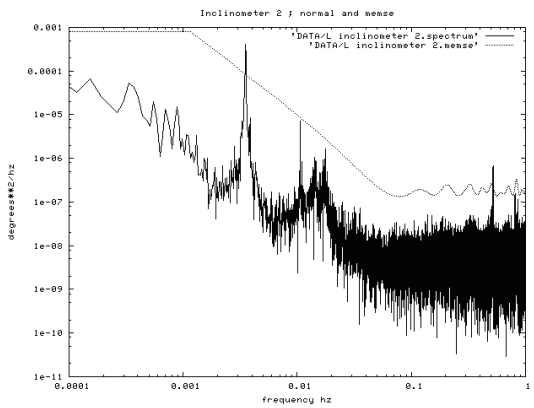

Illustration 62 Lucas inclinometer 2 - comparison of power spectrum and maximum entropy